Modelling co-gasification of plastic waste and lignin in super-critical water using reactive molecular dynamics simulations

Tao Wang[1], Xiangyang Liu*[1], Sihan Huang[1], Waheed Afzal[2], Maogang He [1]

1. Key Laboratory of Thermal Fluid Science and Engineering of MOE, School of Energy and Power Engineering, Xi'an Jiaotong University, Xi'an, 710049, China

2. Chemical & Materials Engineering, School of Engineering, University of Aberdeen, UK.

* Correspondence: lxyyang@mail.xjtu.edu.cn;

Abstract: Supercritical gasification is a promising technology for the utilisation of biomass and plastic wastes. To further understand the synergistic effect of lignin and plastic co-gasification under the influence of supercritical water, the microscopic mechanism of the co-gasification of lignin and plastic in supercritical water was studied using reactive molecular dynamics simulations. The influence of temperature on the evolution behaviour of the carbon chains was also analysed. At low temperatures, lignin cracks slowly, whereas most polyethylene does not crack, and gas production yield is low. The quantity of supercritical water participating in gasification increases with increasing temperature, but there exists an upper limit to this increase. At high temperatures, the main gasification products include H_2, CH_4, CO, and CO_2.

Keywords: Plastic waste; Lignin; Supercritical water; Co-gasification.

1. Introduction

Due to the increase of environmental pressure and depletion of fossil resources, new renewable energy and waste disposal methods are urgently needed [1]. Plastics are widely used in daily life, e.g. in food, transportation, and safety protection. However, plastic products usually consist of long-chain macromolecules that are difficult to degrade under natural conditions. Long-term accumulation of such plastic products can cause serious damage and pollution to the environment [2,3]. Biomass can be used as a source of renewable energy [4]. Lignin is a kind of biomass that can be directly converted into coke, bio-oil, and natural gas [5]. However, the development and utilisation of lignin are not as advanced as those of cellulose and hemicellulose [6].

Pyrolytic gasification is an effective method for the treatment of municipal solid waste. In this regard, supercritical water gasification (SCWG) is considered a promising thermochemical technology for the energy conversion of organic solid waste. SCW is characterized by low viscosity, low mass transfer resistance, good diffusion performance, large heat capacity, and high solubility of most organic compounds, and thus provides a good reaction environment for the co-gasification of biomass and plastics. In the gasification process, as the medium and reactant, SCW can induce macromolecules with low reactivity to participate in the chemical reaction to generate H_2-rich syngas [7,8]. Yan et al., [9] studied the enhancement effect of SCW on scrap tire (ST) depolymerisation, and the results showed that SCW acts both in clusters and as monomers during this process. Moreover, the relative fractions of the SCW clusters and monomers can control the components of the depolymerisation products. Skarmoutsos et al., [10,11] investigated the molecular structure of SC fluids (pure and mixed), demonstrating that local density inhomogeneities occurred in water under supercritical conditions (T>Tc, P>Pc). It can be assumed that local density inhomogeneities in SCW play a significant role in the microscopic mechanism of the gasification process.

From a practical point of view, there are both lignin and plastic in the waste [12-15], and there has been an increasing number of studies on the use of SCW to usefully dispose of plastics and biomass materials in an environment-friendly manner [16-23]. Our group studied the gasification processes of lignin in SCW at nine different temperatures and analysed the cleavage mechanism. The results showed that these processes could generate different numbers of H_2 and CO gas products [20] in different temperatures. We also studied the catalytic SCWG of lignin using different nanocatalysts to understand the degradation mechanism and the path of gas generation. The results showed the different effects of two types of catalysts in accelerating the gasification reaction [21]. Furthermore, Zhao et al., [22] studied the gasification of polystyrene (PS) in SCW with CO_2. The results showed that the liquid composition changed with increasing temperature, and in SCW, the carbon conversion efficiency of PS plastic reached 47.6% at 973 K. Cao et al., [12] experimentally investigated the co-gasification of soda lignin produced from black liquor and various plastics in SCW and reported a synergetic effect in the co-gasification of polyethylene (PE) and soda lignin. The results showed that the addition of soda lignin improved the gasification efficiency.

However, there has been limited research on the microscopic mechanism of the co-gasification of lignin and plastic in SCW. To further elucidate the synergistic effect of lignin and plastic co-gasification and the influence of SCW on their gasification process, in this study, we investigated the co-gasification process of plastic and biomass in SCW by reactive molecular dynamics simulation. β-O-4 lignin and polyethylene, which are the most common substances present in solid waste, were used as lignin and plastics, respectively. Most reactions involved in SCWG, including decomposition, hydrolysis, and steam reforming reactions, are endothermic in nature; therefore, temperature is an important parameter, and higher temperatures favour gasification.

2. Materials and Methods

Molecular dynamics simulation is an effective method to reveal microscopic phenomena that are difficult to observe experimentally and has been widely used in many studies [20-30]. The ReaxFF force field has been successfully used to describe chemical reactions in numerous studies [31-34], such as the decomposition and combustion processes of toluene and cyclic compounds. A version of the force field for C/H/O was adopted in this study, and more details are provided in the supplementary material [35]. The overall system energy can be described by equation (1), which include the following terms: bond energy, pair energy, over-coordinated energy, angle energy, under-coordination energy, valence lone terms energy, penalty energy, two carbons in stability energy, triple bond energy correction, torsion rotation barriers, four-body conjugation term, hydrogen bond interactions, and non-bonded interactions.

$$E_{system} = E_{bond} + E_{lp} + E_{over} + E_{angle} + E_{under} + E_{val} + E_{pen} + E_{coa} + E_{C2} + E_{triple} + E_{tors} + E_{conj} + E_{H-bond} + E_{vdWaals} + E_{Coulomb} \quad (1)$$

In order to verify the accuracy of this method, the density of water at 325 K and 800 K and 57.413MPa were calculated and compared with experimental values [36,37]. The deviations were shown in Table 1, and the results means that the simulation method is reliable.

Table 1. Density of high pressure water and supercritical water.

	T/K	ReaxFF	Expt	Error

ρ (g/cm³)	325	1.0366	1.0107	2.6%
	800	0.2813	0.2681	4.9%

The molecular model of the β-O-4 molecule and polyethylene (PE) was constructed using Material Studio software [38], as shown in Figure 1. To optimise the initial molecular model for validation and obtain a more suitable structure, the density functional theory (DFT) approach was used at the level of the generalised gradient approximation (GGA) with the Becke–Lee–Yan–Parr (BLYP) functional [39]. They are composed of flexible molecules with flexible bonds that exhibit translational, rotational, torsional, and vibrational motion. In the following figures, the hydrogen atoms are represented by blue balls, the carbon atoms are represented by black balls, and the oxygen atoms are represented by red balls.

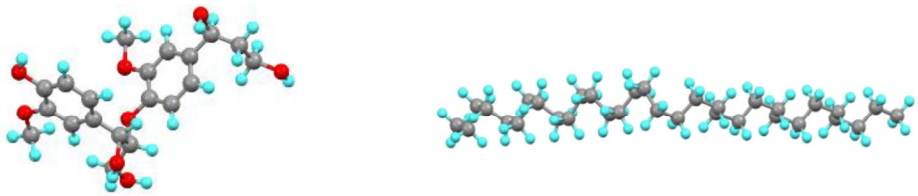

(a) (b)

Figure 1. molecular model. (**a**) β-O-4 molecule; (**b**) polyethylene.

In the reaction process, bond breaking, and bond formation were simulated with bond order. Each pair of atoms connected independently and using the electronegativity equalisation method to evaluate the atomic charges can be used to directly calculate the charge distribution of each region of the system and the total energy [40-42]. Cubic cells were constructed with periodic boundary conditions to establish the initial structure and eliminate surface effects. The optimised structure shown in Figure 2 is an example of a polyethylene-lignin co-gasification system with 7PE and 8 β-O-4 in SCW in a SCW environment with 200 SCW molecules. Many previous studies have shown that increasing temperature increases the reaction rate but does not affect the reaction process [32-35], and Reaxff molecular dynamics simulations usually set a higher temperature to observe chemical reactions on a computational time scale [40,41]. Therefore, in this study, the simulation temperature was set to 2000 K to 5000 K. First, the simulated system was balanced at 325 K. After the simulation system reached stability, it was heated from 325 K to the simulation temperature of 104.48 MPa. Subsequently, each system was simulated for 2 ns to ensure that the reaction time was sufficient. All Reaxff MD simulations were performed using LAMMPS under canonical ensemble (NVT) [43,44].

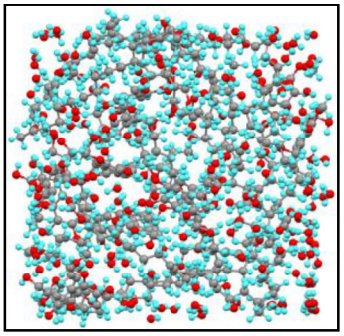

Figure 2. Polyethylene - lignin in SCW system

3. Results and Discussion

To analyse the depolymerisation process, the variations in the C chain fragment in the reaction system were studied by classification as C1, C2, C3-C4, C5-C19 lignin, and PE (Cn denotes carbon chain with n carbon atoms). Figures 3–6 show the change in the number of molecular fragments with different carbon chains in the initial 0.5 ns of simulation time at four different temperatures. It can be concluded from the figures that at 2000 K, only a few polyethylene molecules are broken, while all lignin molecules are broken after 0.1 ns, many molecular fragments with long carbon chains (C5-C19) remain, and the number of fragments with shorter chains is very small. At 3000 K, within 0.5 ns, all the lignin and polyethylene molecules were broken, and the long-carbon-chain (C5-C19) fragments were generated rapidly, which were later broken into shorter-carbon-chain fragments. The number of fragments with shorter carbon chains increased gradually and then stabilized at about 0.1 ns. At 4000 K and 5000 K, the lignin and polyethylene molecules were all broken within 0.01 ns, and the generation of C1, C2, C3-C4 fragments was much faster than at 3000 K, while the generation of C1 fragments at 5000 K exceeded that at 4000 K. At 3000 K, many C5-C19 fragments were rapidly generated. The number of C5-C19 fragments generated at 4000 K was significantly reduced, while that at 5000 K was the lowest. This is because at higher temperatures, the molecules move more rapidly and collisions are more energetic, leading to the fragmentation of longer carbon chains into shorter chains once generated.

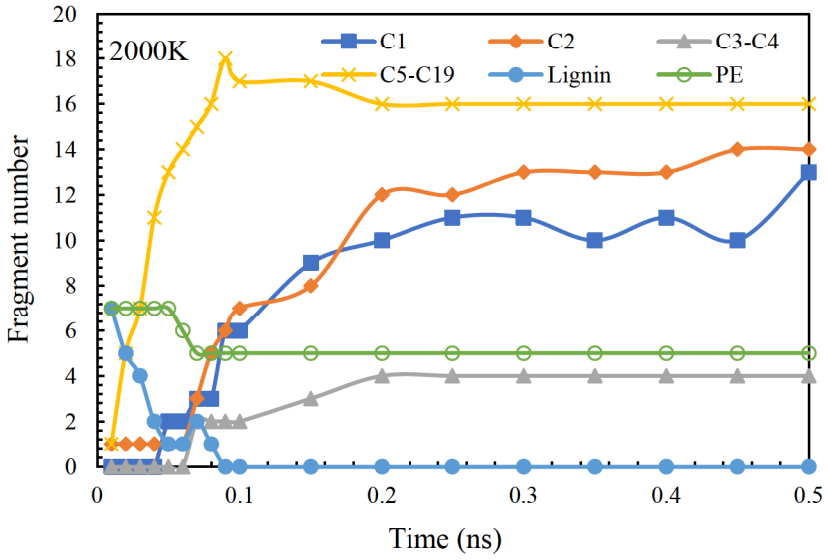

Figure 3. The initial change of different carbon chain fragments at 2000K.

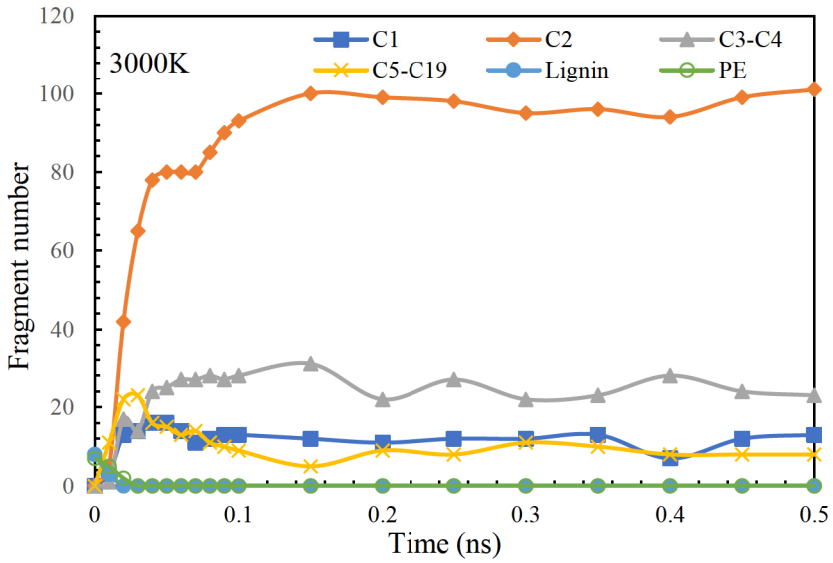

Figure 4. The initial change of different carbon chain fragments at 3000K.

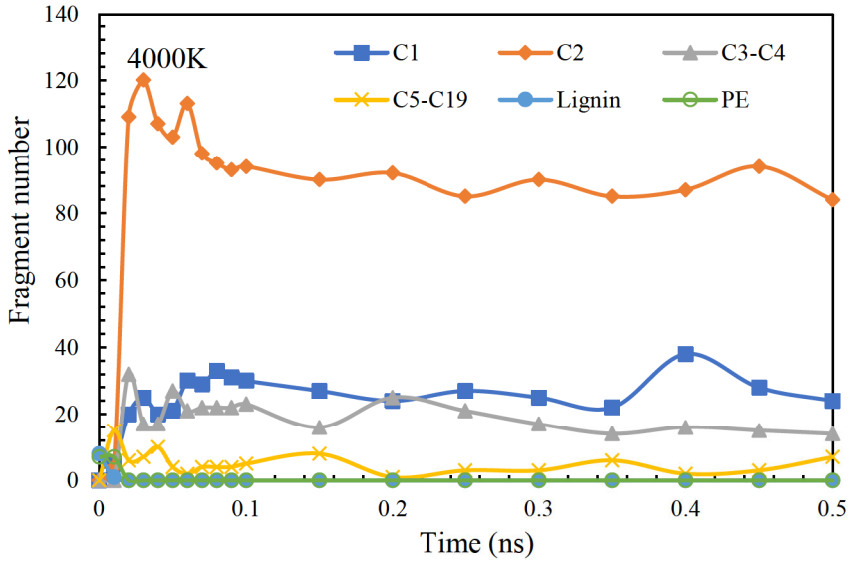

Figure 5. The initial change of different carbon chain fragments at 4000K.

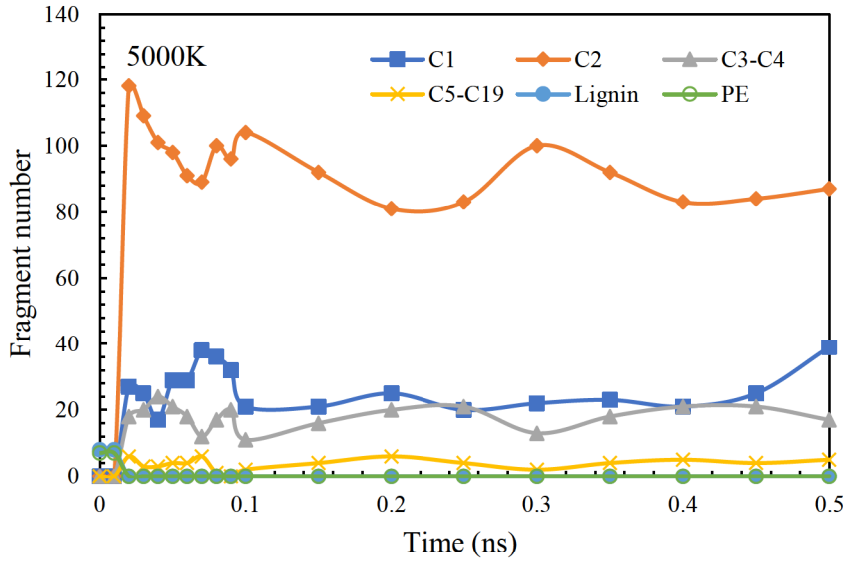

Figure 6. The initial change of different carbon chain fragments at 5000K.

Figure 7 shows the numbers of molecular fragments with different carbon chain lengths at the end of the simulation. It can be concluded that as the temperature increases, the numbers of C1 and C3-C4 fragments increase, while that of C5-C19 fragments decreases. At 2000 K, the number of C2 fragments is small, but when the temperature exceeds 3000 K, the number of C2 fragments increases, and their difference at higher temperatures becomes small, which means that the influence of the change in temperature on the number of C2 is small. At 4000 K and 5000 K, there were almost equal numbers of C5-C19 fragments, and the differences in the carbon chain lengths between the two temperatures were also small.

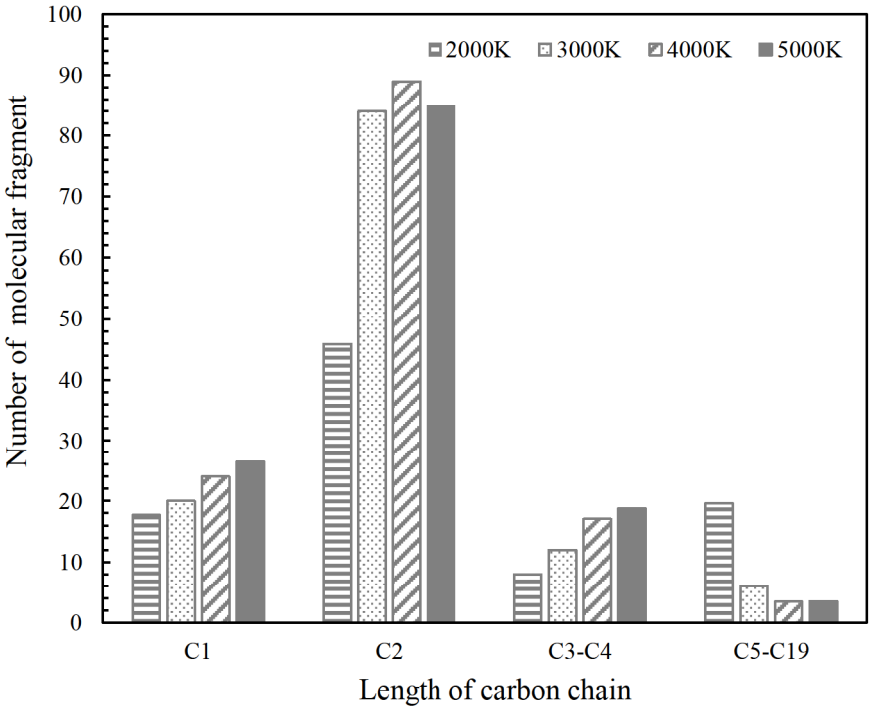

Figure 7. The number of molecular fragments with different length carbon chain at the end of the simulation.

Figure 8 shows the number of SCW molecules that remained and were consumed. It can be concluded that the number of water molecules consumed increases with increasing temperature. Almost no SCW was consumed at 2000 K. The number of water molecules remained constant at 4000 K and 5000 K, indicating that when the temperature reached a limiting value, increasing the temperature had negligible effect on promoting the reaction.

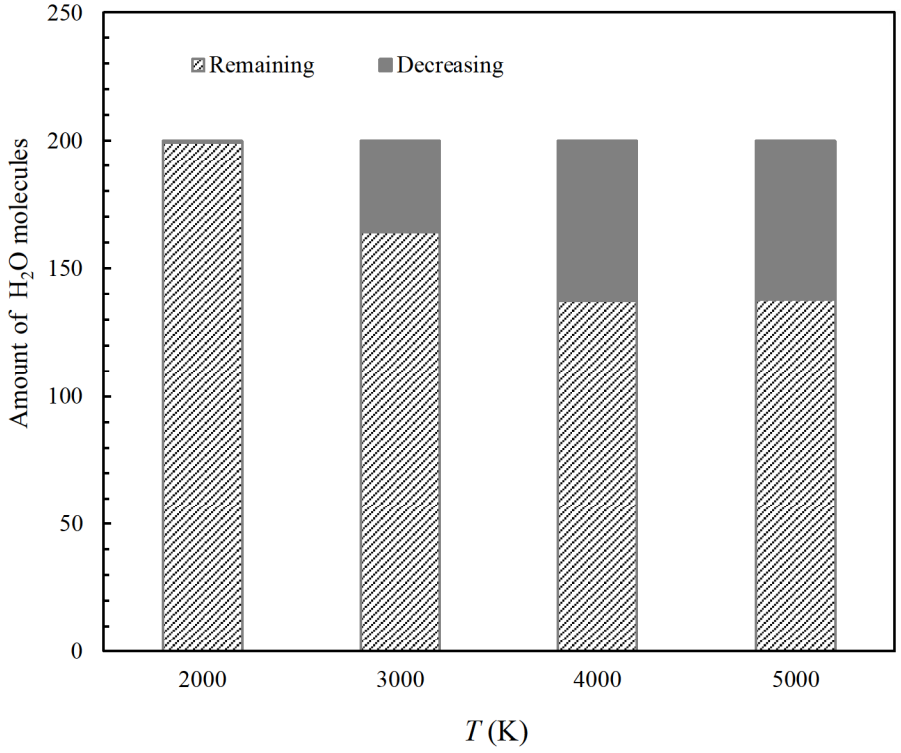

Figure 8. The number of supercritical H_2O left and consumed.

4. Discussion

Many different types of alkanes were generated in the simulation, among which methane was the most abundant, and gasification of PE afforded higher yields of methane than that of lignin, consistent with the results reported by Cao et al [12]. In this study, the main four gas products were shown in Figure 9, including H_2, CO, CO_2, and CH_4, and the number above each column represents the proportions of the four products at the same temperature. It can be concluded from the figure that the yield of gas production was low at 2000 K, and the CO_2 yield was low at all temperatures. The higher the temperature, the more H_2 and CO molecules were produced, consistent with the results reported by Cao et al [12]. However, when the temperature exceeded 4000 K, the number of H_2 and CO molecules changed very little with increasing temperature, indicating that there is an upper limit on the production of H_2 and CO. When the temperature was above 3000 K, the amount of CH_4 decreased with increasing temperature, consistent with the results reported by Cao et al [12]., because CH_4 continued to participate in the cleavage reaction, forming smaller molecules or molecular fragments.

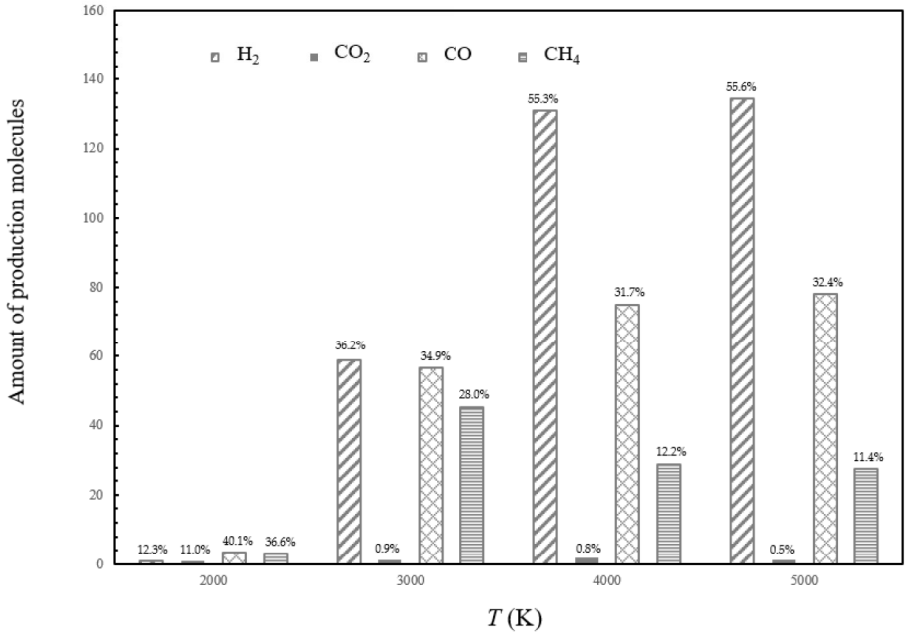

Figure 9. The number of gases produced.

5. Conclusions

In this study, the co-gasification of *β*-O-4 lignin and polyethylene in SCW was examined using the ReaxFF MD method. During the co-gasification process of lignin and polyethylene in SCW, the long-carbon-chain (C5-C19) molecular fragments were first generated, which were subsequently broken into shorter chains. At low temperatures, lignin cracks slowly but completely, whereas most PE remains intact. At high temperatures, a large number of short-chain molecular fragments are produced, and their collisions intensify, making the cracking more rapid and complete. As the temperature increased, the number of C1 fragments increased, while the number of C5-C19 fragments decreases. The number of water molecules consumed with an increase in temperature is limited. At 2000 K, gas production is small, at higher temperatures, gas productions increase apparently, and the order of yield is $H_2 > CO > CH_4 > CO_2$. The production of gases is affected by temperature; as the temperature increases, the production of H_2 and CO increases, but this increase is limited.

Funding: This research was funded by the National Natural Science Foundation of China (No.51936009 and No. 51721004), and Shaanxi Provincial Department of science and technology (NO.2020JQ-907).

References

1. Wang, T., Liu, X., He, M., Zhang., y. Molecular dynamics simulation of thermophysical properties and condensation process of R1233zd(E). Int. J. Refrig. 2020, 112, 341-347.
2. Liu, X., Xue, S., Ikram, R., Zhu, C., Shi, Y., He, M. Improving the viscosity and density of n-butanol as alternative to gasoline by blending with dimethyl carbonate. Fuel. 2021, 286, 119360.
3. Song, F., Wang, Q., Meng, Q., Mu, H., Fan, J. Measurements on the thermal conductivity of three fuel blends containing a biodiesel compound methyl laurate + diesel compounds: n-undecane, n-dodecane, n-tridecane. Thermochim. Acta. 2021, 178986.
4. Cavusoglu, A. H., Chen, X., Gentine, P., Sahin, O. Potential for natural evaporation as a reliable renewable energy resource. Nat. Commun. 2017, 8(1), 617.
5. Dhakshinamoorthy, G. P., Kannappan. P. G., Sevalur. M. P., Sivakumaran. H., Muthamilselvam. R., Ramachandran. S., Arivalagan. P. Extraction methodology of lignin from biomass waste influences the quality of bio-oil obtained by solvothermal depolymerization process. Chemosphere. 2021, 293, 133473.
6. Suresh, S., V, Viswanathan, Angamuthu, M., Dhakshinamoorthy, G. P., Gopinath, K. P., Bhatnagar, A. Lignin waste processing into solid, liquid, and gaseous fuels: a comprehensive review. Biomass Convers. Biorefin. 2021,1-39.

7. Ding, W., Shi, J., Wei, W., Cao, C., Jin, H.A molecular dynamics simulation study on solubility behaviors of polycyclic aromatic hydrocarbons in supercritical water/hydrogen environment. Int. J. Hydrog. Energ. 2020, 46, 2899-2904.
8. Wang, C., Zhu, C., Huang, J., Li, L., Jin, H. Enhancement of depolymerization slag gasification in supercritical water and its gasification performance in fluidized bed reactor. Renew. Energ. 2020, 168, 829-837.
9. Yan, S., Xia, D., Xuan, W. New insight into enhancement effect of supercritical water on scrap tire depolymerization: a study based on reaxff-md simulation and dft method. Fuel Process. Technol. 2020, 200, 106309.
10. Skarmoutsos, I., Samios, J. Local density augmentation and dynamic properties of hydrogen-and non-hydrogen-bonded supercritical fluids: a molecular dynamics study. J. Chem. Phys. 2007, 126(4), 391-72.
11. Skarmoutsos, I., Dellis, D., Samios, J. The effect of intermolecular interactions on local density inhomogeneities and related dynamics in pure supercritical fluids. a comparative molecular dynamics simulation study. J. Phys. Chem. B. 2009,113(9), 2783-2793.
12. Cao, C., Bian, C., Wang, G., Bai, B., Xie, Y., Jin, H. Co-gasification of plastic wastes and soda lignin in supercritical water. Chem. Eng. J. 2020, 388, 124277.
13. Jin, W., Shen, D., Liu, Q., Xiao, R. Evaluation of the co-pyrolysis of lignin with plastic polymers by TG-FTIR and Py-GC/MS. Polym. Degrad. Stab. 2016, 133, 65-74.
14. Qian, M., Lei, H., Villota, E., Zhao, Y., Huo, E., Wang, C., Mateo, W., Zou, R. Enhanced production of renewable aromatic hydrocarbons for jet-fuel from softwood biomass and plastic waste using hierarchical ZSM-5 modified with lignin-assisted re-assembly. Energy Convers. Manage. 2021, 236, 114020.
15. Zhang, H., Xiao, R., Nie, J., Jin, B., Shao, S., Xiao, G. Catalytic pyrolysis of black-liquor lignin by co-feeding with different plastics in a fluidized bed reactor. Bioresour. Technol. 2015, 192, 68-74.
16. Vivek, P., Sushil, A., Phillip, C. Co-pyrolysis of lignin and plastics using red clay as catalyst in a micro-pyrolyzer. Bioresour. Technol. 2018, 270, 311-319.
17. Weber, R. S., Ramasamy, K. K. Electrochemical oxidation of lignin and waste plastic. ACS Omega. 2020, 5(43), 27735-27740.
18. Jin, H.; Wang, Y.; Wang, H.; Wu, Z.; Li, X. Influence of Stefan flow on the drag coefficient and heat transfer of a spherical particle in a supercritical water cross flow. Phys. Fluids. 2021, 33(2), 023313.
19. Li, X.; Wu, Z.; Wang, H.; Jin, H. The effect of particle wake on the heat transfer characteristics between interactive particles in supercritical water. Chem. Eng. Sci. 2022, 247, 117030.
20. Liu, X., Wang, T., Chu, J., He, M., Li，Q., Zhang， Y. Understanding lignin gasification in supercritical water using reactive molecular dynamics simulations. Renew. Energ. 2020, 161, 858-866.
21. Wang, T., Liu, X., Liu, H., He, M. Synergistic effect of supercritical water and nano-catalyst on lignin gasification. Int. J. Hydrogen Energ. 2021，46, 34626-34637.
22. Zhao, S.; Wang, C.; Bai, B.; Jin, H.; Wei, W. Study on the polystyrene plastic degradation in supercritical water/CO_2 mixed environment and carbon fixation of polystyrene plastic in CO_2. J. Hazard. Mater. 2022, 421, 126763.
23. Song, F., Niu, H., Fan, J., Chen, Q., Wang, G., Liu, L. Molecular dynamics study on the coalescence and break-up behaviors of ionic droplets under dc electric field. J. Mol. Liq. 2020, 312. 113195.
24. Li, Q., Deng, X., Liu, Y., Cheng, Q., Liu, C. Gelation of waxy crude oil system with ethylene-vinyl acetate on solid surface: a molecular dynamics study. J. Mol. Liq. 2021, 331. 115816.
25. Cai, S., Wu, C., Li, X., Li, Q. Effects of lubricant on evaporation and boiling processes of r1234ze(e): a molecular dynamics study. Appl. Therm. Eng. 2021, 193. 117009.
26. Li, Q., Wang, M., Liang, Y., Lin, L., Fu, T., Wei, P. Molecular dynamics simulations of aggregation of copper nanoparticles with different heating rates. Phys. E (Amsterdam, Neth.), 2017, 90, 137-142.
27. Wang, T., Liu, X., Chu, J., Shi, Y., Li, J., He, M. Molecular dynamics simulation of diffusion and interaction of [bmim][tf2n] + hfo-1234yf mixture. J. Mol. Liq. 2020, 312, 113390.
28. Liu, X., Zong, X., Xue, S., Liu, H., He, M. Molecular structure and transport of ionic liquid confined in asymmetric graphene-coated silica nanochannel. J. Mol. Liq. 2022, 345, 117869.
29. Wang, T., Liu, X., He, M., Zhang, Y. Molecular dynamics simulation of thermophysical properties and condensation process of r1233zd(e). Int. J. Refrig. 2020, 112(5).
30. Liu, X., Wang, T., He, M. Investigation on the condensation process of hfo refrigerants by molecular dynamics simulation. J. Mol. Liq. 2019, 288, 111034.
31. Singh S K, Srinivasan S G, Neek-Amal M, Costamagna S, Van Duin A C T, F. Peeters M, Thermal properties of fluorinated graphene. Phys Rev B. 2013, 87(10) 104114.
32. Zhu, C., Susanna, M., Mathew, A. P. Cellulose nanofiber-graphene oxide biohybrids: disclosing the self-assembly and copper-ion adsorption using advanced microscopy and reaxff simulations. Acs Nano acsnano. 2018, 8b02734.
33. Achtyl, J. L.; Unocic, R. R.; Xu, L.; Cai, Y.; Raju, M.; Zhang, W.; Sacci, R. L.; Vlassiouk, I. V.; Fulvio, P. F.; Ganesh, P.; Wesolowski, D. J.; Dai, S.; Van Duin, A. C. T.; Neurock, M.; Geiger, F. M. Aqueous Proton Transfer Across Single-Layer Graphene. Nat. Commun, 2015, 6. 6539.
34. Wang, T., Liu, X., Liu. H., He, M., Synergistic effect of supercritical water and nano-catalyst on lignin gasification. Int. J. Hydrogen Energy. 2021, 46(70), 0360-3199.
35. Senftle, T. P., Hong, S., Islam, M. M., Kylasa, S. B., Zheng, Y., Shin, Y. K.The reaxff reactive force-field: development, applications and future directions. Npj Comput. Mathematic. 2016, 2, 15011.
36. Soleymanibrojeni, M., Shi, H., Liu, F., Han, E. H. Atomistic simulations of epoxy/water/aluminum systems using the reaxff method. Comput Mater Sci. 2019, Vol. 173, pp.109424.

37. Lemmon EW, Bell IH, Huber ML, McLinden MO. NIST reference fluid thermodynamic and transport properties database e REFPROP, Version 10.0. Standard reference data program. National Institute of Standards and Technology Gaithersburg; 2017.
38. Delley, B. From molecules to solids with the DMol3 approach. J Chem Phys. 2000, Vol. 113, pp.7756-7764.
39. Lee C, Yang W, Parr RG. Development of the Colle–Salvetti correlation-energy formula into a functional of the electron density. Phys Rev B. 1988;37(2):785–9.
40. Ashraf, C., Shabnam, S., Jain, A., Xuan, Y., van Duin, A.C.T. Pyrolysis of binary fuel mixtures at supercritical conditions: A ReaxFF molecular dynamics study, Fuel. 2019, 235. 194–207.
41. Kimberly Chenoweth, Adri C. T. van Duin, and William A. Goddard. ReaxFF Reactive Force Field for Molecular Dynamics Simulations of Hydrocarbon Oxidation. J. Phy. Chem. A. 2008 112 (5), 1040-1053.
42. Landis, C. R., Cleveland, T., Firman, T. K. Valence Bond Concepts Applied to the Molecular Mechanics Description of Molecular Shapes. 3. Applications to Transition Metal Alkyls and Hydrides. J. Am. Chem. Soc. 1998, 120(11), 2641–2649.
43. Yan, S., Xia, D., Zhang, X., Jiang, B. (2019). A complete depolymerization of scrap tire with supercritical water participation: a molecular dynamic simulation study. J. Waste Manage., 93, 83-90.
44. Jiang, B., Xia, D., Xie, Y., Liu, X. (2019). Effect of the molecular structure of volatile organic compounds on atmospheric nucleation: a modeling study based on gas kinetic theory and graph theory. Atmos. Environ. 213, 215-222.